

## THERMOGRAVIMETRY AND EVOLVED GAS ANALYSIS OF THE REDUCTION OF HEMATITE ( $\text{Fe}_2\text{O}_3$ ) WITH GRAPHITE

THOMAS SZENDREI and P.C. VAN BERGE

*Chemistry Department, Rand Afrikaans University, P.O. Box 524, Johannesburg 2000 (Republic of South Africa)*

(Received 14 July 1980)

### ABSTRACT

A simple interface is described between a Mettler thermoanalyzer and a quadrupole mass spectrometer which permits simultaneous thermal analysis and evolved gas analysis at atmospheric pressure without compromising the normal operation of the thermoanalyzer. The application of the combination is described with respect to the reduction of hematite ( $\text{Fe}_2\text{O}_3$ ) with graphite. Direct experimental evidence is provided for the reaction model wherein each iron oxide phase is converted in turn to the next lower one and it is shown that reduction proceeds under a  $\text{CO}-\text{CO}_2$  atmosphere which is in equilibrium with the various oxide phases. It is further shown that in the presence of  $\text{Na}_2\text{CO}_3$  the CO concentration is enhanced. It is concluded that the known catalytic effect of sodium (and other alkalis) on solid direct reduction derives primarily from its acceleration of the rate of carbon gasification.

### INTRODUCTION

The combined operation of vacuum thermal balances and mass spectrometers has been well documented [1,2]; descriptions of TA-MS combinations operating at ambient pressures, on the other hand, are less common [3]. Operation at these pressures would evidently greatly enhance the utility of the combination since in many applications it is desirable to carry out thermal analysis in atmospheres which may be oxidising, reducing or self-generated. This paper describes a simple interface between a Mettler thermoanalyzer and a quadrupole mass spectrometer which permits simultaneous TA and evolved gas analysis (EGA) at atmospheric pressure without compromising the normal TA operation (TG, DTG, DTA) or the nature of the furnace atmosphere. The application of the combination is discussed with respect to the reduction of hematite ( $\text{Fe}_2\text{O}_3$ ) with solid carbon.

The  $\text{Fe}_2\text{O}_3/\text{C}$  reaction system is not only of obvious technological significance for the production of sponge iron, but it also poses a number of problems of scientific interest.

In the first place, solid direct reduction comprises a complex sequence of overlapping reactions. The overall extent of reduction is determined by the following reactions [15].



According to this cyclic mechanism, carbon must pass through the intermediate stage of CO formation prior to reaction with iron oxides. The initial formation of CO is ascribed to a number of causes: adsorbed oxygen; dissociation of iron oxides; direct solid—solid reaction between carbon and hematite ( $\text{Fe}_2\text{O}_3$ ). The gas—carbon and gas—oxide reactions proceed in parallel and influence each other through the composition of the resulting CO—CO<sub>2</sub> atmosphere. It is evident that without prior knowledge of the composition of this atmosphere, a theoretical interpretation of the kinetics and mechanism of reduction would be greatly hindered. For this reason EGA has an essential contribution to make to the study of the hematite/carbon reaction system.

Previous attempts to determine the composition of the reaction atmosphere included mass spectrometry [4] of gases from a sample kept at  $5 \times 10^{-4}$  torr, and the collection in adsorption columns of CO<sub>2</sub> present in the effluent gas stream from a reactor [5,6]. Direct in situ measurements of reaction product gases during reduction at atmospheric pressure have not been reported.

Secondly, solid direct reduction is of theoretical interest in the wider context of gas—solid reactions. It affords a system of two coupled gas—solid reactions on which, in contrast to the very extensive modelling studies that have been performed on single gas—solid reactions, very little theoretical work has been done. Szekely et al. [7] have shown that in such systems the complexity of the resulting rate equations generally compels their evaluation by numerical methods. They further showed that in two asymptotic cases — when either one of the two coupled reactions proceeds very much faster than the other one — the governing equations simplify to that for a single gas—solid reaction. By measurement of the CO/CO<sub>2</sub> ratio it would be possible to determine whether reduction proceeds in one of the asymptotic regions. If required, it would also be possible to monitor the approach to one of these regions as reduction conditions are varied (e.g. crucible and sample geometry, carbon particle size, nature of carbon, catalysts).

Thirdly, it has been noted [8–11] that additions of alkali salts generally catalyse the reduction of iron oxides by solid carbon. Detection of possible changes in the composition of reduction atmosphere may contribute to an understanding of the catalytic effect. For this reason EGA was also performed on a reduction mixture containing sodium carbonate.

## EXPERIMENTAL

### *Thermal analyser—mass spectrometer system*

A Mettler thermoanalyzer was linked to an EAI Quad 300 mass spectrometer via a two-stage sampling system. The main components of the system

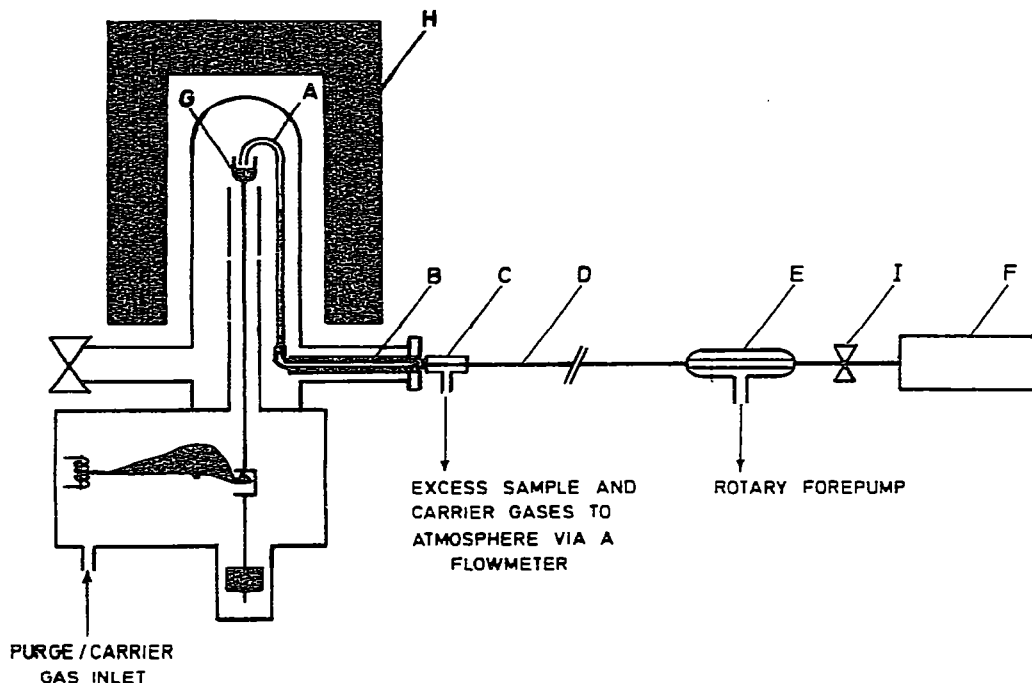


Fig. 1. Schematic diagram of the thermoanalyzer—mass spectrometer combination. A, Silica glass sampling tube; B, heated silica glass transfer tube; C, bypass and sampling capillary; D, PTFE capillary tubing; E, Watson—Biemann molecular separator; F, quadrupole gas analyzer; G, sample; H, furnace; I, shut-off valve.

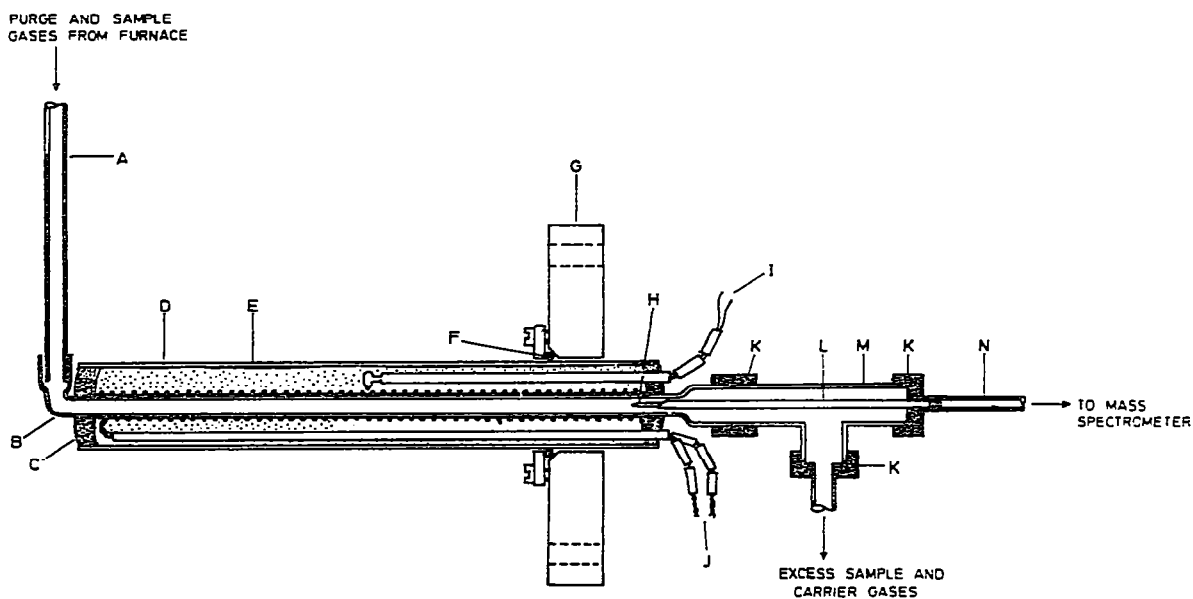


Fig. 2. Details of gas sampling system. A, Silica glass sampling tube; B, silica glass transfer tube; C, airtight refractory cement plug; D, silica glass sheath; E, ceramic fibre insulation; F, 'O'-ring seal; G, brass flange; H, glass sampling capillary; I, thermocouple; J, heater windings; K, 'Swagelok' unions; L, stainless steel sheath; M, glass 'T' piece; N, 1.5 mm PTFE capillary.

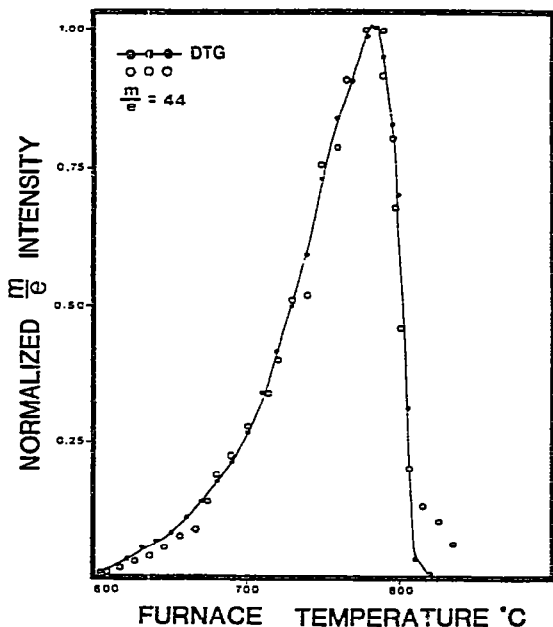


Fig. 3. Decomposition of  $\text{CaCO}_3$  studied by the TA-MS combination. Sample, 100 mg  $\text{CaCO}_3$  (Hopkin and Williams); sample holder, cylindrical alumina crucible; furnace atmosphere, flowing argon ( $50 \text{ ml min}^{-1}$ ); heating rate,  $6^\circ\text{C min}^{-1}$ .

are indicated in Fig. 1. Details of the sampling system are shown in Fig. 2.

A small fraction of the furnace purge gas stream was drawn through a capillary H (Fig. 2) and conducted to a pre-vacuum inlet system comprising a 1.5 l stainless steel flask linked to a high-speed rotary pump ( $53 \text{ l min}^{-1}$ ). A pre-vacuum pressure of approximately 0.1 torr was generally maintained during combined TA/MS operation. A molecular ("pinhole") leak reduced the pressure to  $10^{-6}$  torr or less in the mass spectrometer ioniser. A unique feature of the present system is the siting of the sampling tube A (Fig. 1) inside the furnace with its tip in the sample holder. By constraining the furnace purge gas to exit through this tube, a rapid and efficient collection of thermal analysis off-gases was achieved. The lack of discernible delay in the mass spectrometer response and the direct proportionality between signal strength and the rate of gas release (DTG) is demonstrated in Fig. 3.

### Materials

Hopkin and Williams-precipitated red ferric oxide (approximately 98%  $\text{Fe}_2\text{O}_3$ ) and spectrographic graphite ( $104\text{--}144 \mu\text{m}$ ) from Union Carbide were used for the preparation of reduction mixtures. A thorough characterization of these materials has been given elsewhere [11].

### Procedure

Reduction samples comprised hematite and graphite mixed in the molar ratio 1 : 2.5. The sample holder used was a cylindrical alumina crucible

(height 20 mm, diameter 16 mm) sitting directly on a Pt/Pt-10% Rh thermocouple. The sample was heated at  $8^{\circ}\text{C min}^{-1}$  in flowing argon ( $50\text{ ml min}^{-1}$ ) at atmospheric pressure (84 kPa). Furnace temperature, TG and DTG curves were recorded on a strip chart. The reaction atmosphere was continuously sampled and conducted to the mass spectrometer. Its composition was scanned at 0.3 s intervals in the  $m/e$  range 1-50, and the peaks were displayed on an oscillograph. When required, the display was transferred onto an oscillographic recorder for the identification of  $m/e$  values and relative intensities.  $m/e$  values of 12( $\text{C}^+$ ), 14( $\text{CO}^{2+}$ ,  $\text{N}^+$ ), 16( $\text{O}^+$ ), 28( $\text{N}_2^+$ ,  $\text{CO}^+$ ), 32( $\text{O}_2^+$ ) and 44( $\text{CO}_2^+$ ) were selected for the calculation of CO and  $\text{CO}_2$  relative intensities, taking into account the contributions to the  $m/e = 28$  peak from background  $\text{N}_2$  as well as from the fragmentation of  $\text{CO}_2$ .

## RESULTS

The results of a combined DTG-EGA investigation of the reaction of  $\text{Fe}_2\text{O}_3 + 2.5\text{ C}$  in the temperature range  $800\text{--}1150^{\circ}\text{C}$  are presented in Fig. 4(a). Both techniques reveal a complexity of features which is discussed in the following section. Figure 4(b) portrays reduction in the presence of  $\text{Na}_2\text{CO}_3$  added as a powder to a premixed reduction mixture. It is evident from the DTG curve that  $\text{Na}_2\text{CO}_3$  has a catalytic influence on reduction. The

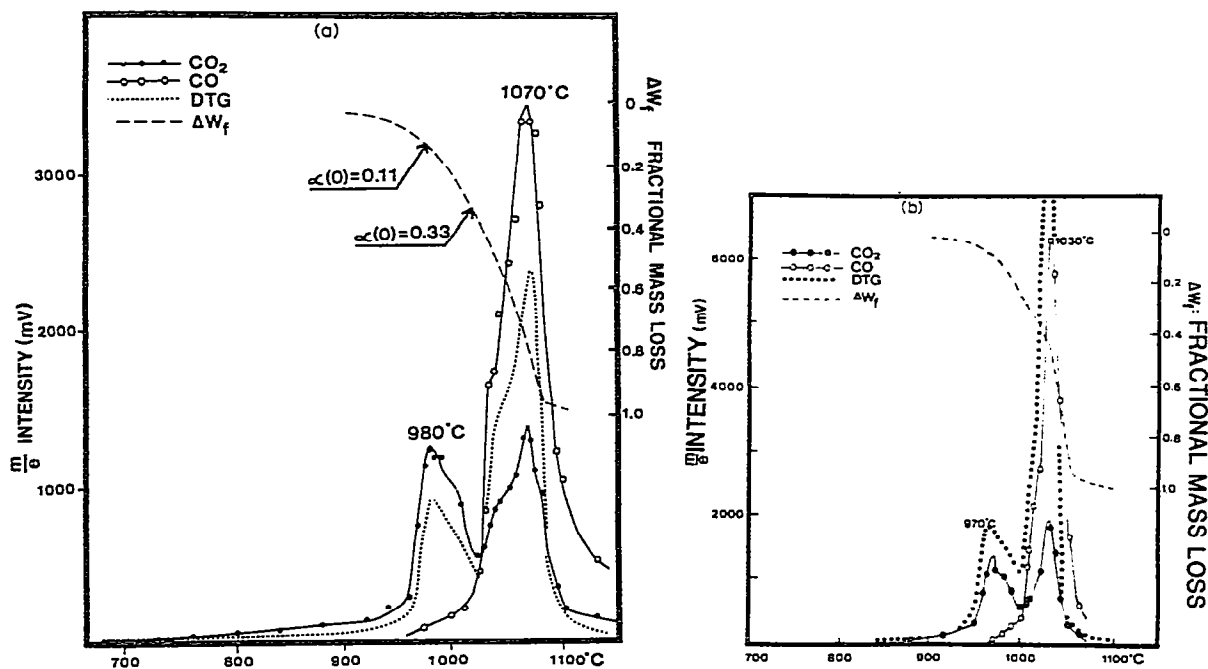


Fig. 4. (a) TA and EGA of the reduction of hematite with graphite. Sample, 80 mg  $\text{Fe}_2\text{O}_3 + 15\text{ mg C}$ ; furnace atmosphere, argon ( $50\text{ ml min}^{-1}$ ); heating rate,  $8^{\circ}\text{C min}^{-1}$ . Significance of  $\alpha(0)$  is explained in text.  $\Delta W_f$  denotes fractional mass loss. (b) TA and EGA of the reduction of hematite with graphite in the presence of sodium. Sample, 80 mg  $\text{Fe}_2\text{O}_3 + 15\text{ mg C} + 1.2\text{ mg Na}_2\text{CO}_3$ . Other experimental details as for Fig. 4(a).

rate of mass loss is higher and the reaction goes to completion at lower temperatures. Except for differences of detail, the overall features of reduction are, however, not altered by the presence of  $\text{Na}_2\text{CO}_3$ . In both cases reduction is characterised by two distinct temperature regions of reaction and widely varying rates of mass loss.

## DISCUSSION

EGA and DTG provide a clear demonstration of the multi-stage nature of reduction, the stages being distinguished by large variations of relative CO,  $\text{CO}_2$  intensities [Fig. 4(a)]. At the start of reduction little or no CO is observed (the estimated error being larger than the calculated value of  $\text{CO}^*$ ). CO first appears in significant concentrations in the vicinity of the maximum of the first DTG peak, and increases particularly rapidly at the onset of the reduction stage associated with the second DTG peak. Relative to CO, the concentration of  $\text{CO}_2$  decreases continuously.

A consideration of the variation of relative CO,  $\text{CO}_2$  intensities suggests that the reduction stages may be identified with the sequential reduction of hematite ( $\text{Fe}_2\text{O}_3$ ) to metallic iron in three steps commensurate with the oxidation states of the iron oxide phases. The three reduction steps with their associated equilibrium CO concentrations are given in Table 1.

It is evident from Fig. 4(a) that the experimentally measured  $\text{CO}/\text{CO}_2$  ratio varies in the direction and approximately in proportion to the calculated values given in Table 1 for reactions I, II and III. It is therefore concluded that, at least to a first approximation, the reduction of hematite takes place in accordance to the mechanism outlined by eqns. (1)–(4) and under a  $\text{CO}-\text{CO}_2$  atmosphere which is in equilibrium with the successive iron oxide phases.

Assuming the validity of the above conclusion, the end points of stages I and II were calculated from the TG data. They are indicated on Fig. 4(a) as  $\alpha(0)$  or fraction of bound oxygen removed, being 0.11 at the end of stage I and 0.33 at the end of stage II. Turning points on the DTG curve are seen to occur in the vicinity of transitions from one reduction stage to another. At these points large changes of relative CO,  $\text{CO}_2$  concentrations also occur. EGA therefore provides a clear interpretation of the DTG profile for solid

TABLE 1

Variation of CO concentration during reduction of hematite

Reaction	Equilibrium CO(%)			Ref.
	1200 K	1300 K	1400 K	
I. $3 \text{Fe}_2\text{O}_3 + \text{CO} \rightarrow 2 \text{Fe}_3\text{O}_4 + \text{CO}_2$	$<10^{-2}$	$<10^{-2}$	$<10^{-2}$	12
II. $\text{Fe}_3\text{O}_4 + \text{CO} \rightarrow 3 \text{FeO} + \text{CO}_2$	20.2	16.0	14.8	13
III. $\text{FeO} + \text{CO} \rightarrow \text{Fe} + \text{CO}_2$	66.8	70.1	73.0	13
IV. $\text{C} + \text{CO}_2 \rightarrow 2 \text{CO}$	97.3	>99	>99	14

direct reduction of hematite. It is determined by the sequential transformation of  $\text{Fe}_2\text{O}_3$  to Fe.

The existence of the three reduction steps identified above has previously been surmised, but not unambiguously demonstrated. Rao [15] reported steps II and III; at temperatures in excess of  $947^\circ\text{C}$  only step III was clearly observed. Fruehan [6] analysed his results by combining the first two steps:  $\text{Fe}_2\text{O}_3$  is reduced directly to FeO.

Based on EGA and DTG, the following points may be noted about the reduction of  $\text{Fe}_2\text{O}_3$ .

The reduction of  $\text{Fe}_2\text{O}_3$  to  $\text{Fe}_3\text{O}_4$  is rapid, viz. the rate of mass loss/unit mass of oxygen is high.

The occurrence of the maximum rate of this reaction step at its end point, suggesting that this step is of an autocatalytic nature, has already been discussed elsewhere [11]. The conversion of  $\text{Fe}_3\text{O}_4$  to FeO, on the other hand, proceeds at a much slower rate. This is indicated by the diminishment of the DTG peak height despite the continuously increasing reaction temperature. The onset of wüstite reduction is extremely rapid — both DTG and CO peak heights at least double in a narrow temperature interval of  $5^\circ\text{C}$ . This is possibly the result of autocatalysis due to the rapid nucleation and spread of metallic iron. The autocatalytic nature of wüstite reduction was inferred by Rao [15,16] on different grounds.

In the presence of  $\text{Na}_2\text{CO}_3$  the reduction of hematite undergoes two major changes [Fig. 4(b)]. Firstly, the rate of reduction — particularly of the  $\text{FeO} \rightarrow \text{Fe}$  step — is greatly enhanced. Secondly, there is a concomitant increase in the production of CO relative to  $\text{CO}_2$ .

The second point is illustrated in Fig. 5 which displays the variation of the CO/ $\text{CO}_2$  ratio with extent of reduction. Fractional reduction values were calculated from the TG data after subtraction of the mass loss associated with the first two stages of reduction. Data points for uncatalysed reduction were

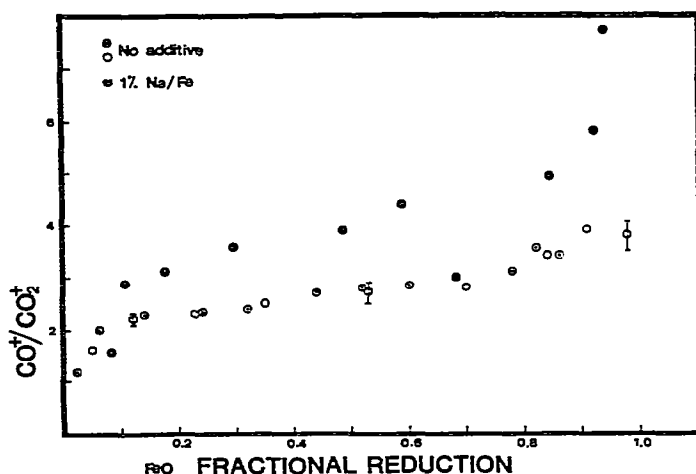


Fig. 5. Variation of reaction atmosphere during reduction of wüstite FeO. Mass loss values have been converted to reflect fractional reduction values. Vertical bars indicate counting statistic errors.

combined from two tests. The scatter of these points, together with the estimate for the errors associated with them, gives an indication of the range of uncertainty in the calculated values of  $\text{CO}/\text{CO}_2$ . This is seen to be much less than the separation between the curves for catalysed and uncatalysed reductions. It should be noted that the calculated  $\text{CO}/\text{CO}_2$  ratios are not absolute values since the calculation does not include corrections for molecular mass selection effects in the sampling technique and for the variation of detector sensitivity with ionic mass.

Examination of Fig. 5 reveals two notable features. These are that (1) the  $\text{CO}/\text{CO}_2$  ratio is essentially constant over a large fraction of uncatalysed reduction, and (2) sodium carbonate enhances this ratio significantly.

It seems reasonable to identify the constant  $\text{CO}/\text{CO}_2$  ratio with the equilibrium gas composition over  $\text{FeO}-\text{Fe}$ . It follows then that when  $\text{Na}_2\text{CO}_3$  is present in the reduction mixture the composition of the reduction atmosphere shifts away from this equilibrium and may even approach equilibrium with graphite ( $\text{CO} > 90\%$ ) in the end stages of reduction. Potassium [9] and other heavy alkalis [10] have been reported to be much better catalysts than sodium for reduction reactions. It is probable therefore that for these alkalis the gas composition would more closely approach the carbon/gas equilibrium at all stages of wüstite reduction.

The above observations lead to two main conclusions. In the first place, it is clear that the catalytic effect of sodium (and probably of other alkalis too) on solid direct reduction derives primarily from its enhancement of the carbon gasification rate. It has been shown [17] that this effect may be interpreted in terms of the uptake of alkalis in the lattice of graphite.

The second conclusion relates to the theoretical treatment of solid direct reduction as a system of coupled gas-solid reactions. Following Szekely et al. [7], the kinetic analysis of reduction may be simplified when the relative rates of the coupled reactions, iron oxide-gas and carbon-gas, are taken into account. It is clear from gas analysis that the rate-limiting reaction for uncatalysed reduction is the gas-carbon reaction. The reduction reactions are very much faster and determine the composition of the reaction atmosphere. The overall kinetics of reduction may then be interpreted in one of the asymptotic regions where only the carbon-gas reaction need be considered. In the presence of sodium, reduction proceeds under mixed control where both reactions (1) and (2) influence the rate of reduction. It may be possible, however, to simplify the analysis by the use of heavier alkalis. These catalysts would increase the CO concentration and the wüstite-gas reaction may become rate-limiting.

#### ACKNOWLEDGEMENT

T.S. thanks the Anglo American Corporation of South Africa for laboratory facilities and financial assistance.



## REFERENCES

- 1 E.K. Gibson, *Thermochim. Acta*, 5 (1973) 243.
- 2 L.W. Collins and E.K. Gibson, *Thermochim. Acta*, 11 (1975) 177.
- 3 M.M. von Moos, G. Kahr and A. Rub, *Thermochim. Acta*, 20 (1977) 387.
- 4 T.S. Yun, *Trans. Am. Soc. Met.*, 54 (1961) 129.
- 5 R. Eck, *Berg Huettenmaenn. Monatsh.*, 113 (1968) 11.
- 6 R.J. Fruehan, *Met. Trans. B*, 8B (1977) 279.
- 7 J. Szekely, J.W. Evans and H.Y. Sohn, *Gas Solid Reactions*, Academic Press, New York, 1976, p. 179.
- 8 G.C. Williams and R.A. Ragatz, *Ind. Eng. Chem.*, 28 (1936) 130.
- 9 S.S. Lisnyak and G.I. Chufarov, *Dokl. Akad. Nauk S.S.S.R.*, 126 (1959) 831.
- 10 M.G. Zhuravleva, G.I. Chufarov and L.G. Kromykh, *Dokl. Akad. Nauk S.S.S.R.*, 135 (1960) 385.
- 11 Thomas Szendrei, Ph.D. Thesis, Rand Afrikaans University, 1977.
- 12 JANAF Thermochemical Tables, National Bureau of Standards, 1965-1968.
- 13 P. Vallet and P. Raccach, *Mem. Sci. Rev. Met.*, 62 (1965) 1.
- 14 David R. Gaskell, *Introduction to Metallurgical Thermodynamics*, Scripta Publishing Company, New York, 1973.
- 15 Y.K. Rao, *Met. Trans.*, 2 (1971) 1439.
- 16 Y.K. Rao, *Chem. Eng. Sci.*, 29 (1974) 1435.
- 17 T. Szendrei and P.C. van Berge, *J. Catal.*, 59 (1979) 1.